Electronic Supplementary Material (ESI) for Physical Chemistry Chemical Physics.
This journal is © the Owner Societies 2017

Supplementary Information

Type-inversion as Working Mechanism of High Voltage MAPbBr$_3$(Cl)-Based Halide Perovskite Solar Cells

Nir Kedem, Michael Kulbak, Thomas M. Brenner, Gary Hodes and David Cahen**

Materials and Interfaces, Weizmann institute of Science, Rehovot, 7610001, Israel

E-mail: david.cahen@weizmann.ac.il; gary.hodes@weizmann.ac.il

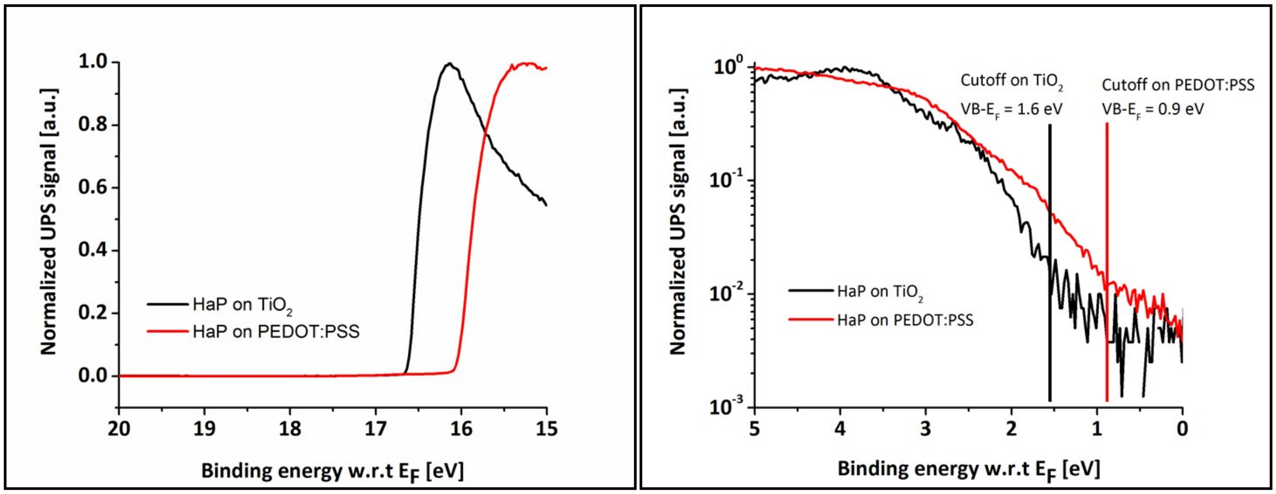

Figure S1. UPS spectra of MAPbBr$_3$(Cl) on TiO$_2$ and on PEDOT:PSS. Left: UPS onset, showing the sample WF = 4.5 – 4.6 eV on TiO$_2$ and 5.1 – 5.2 eV on PEDOT:PSS. Right: UPS cut-off, showing the Fermi level position (E$_F$ at 0 eV binding energy). MAPbBr$_3$(Cl) VBM is at 1.6 ± 0.1 eV below the Fermi level on TiO$_2$ and on PEDOT:PSS at 0.9 eV.

As mentioned in the main text, 4 different UPS measurements of the WF were made, 2 on bare substrates and 2 with the HaP deposited on the substrates. Since the measurement values were the same within the experimental error range we show only the UPS spectra of the HaP on the substrates.

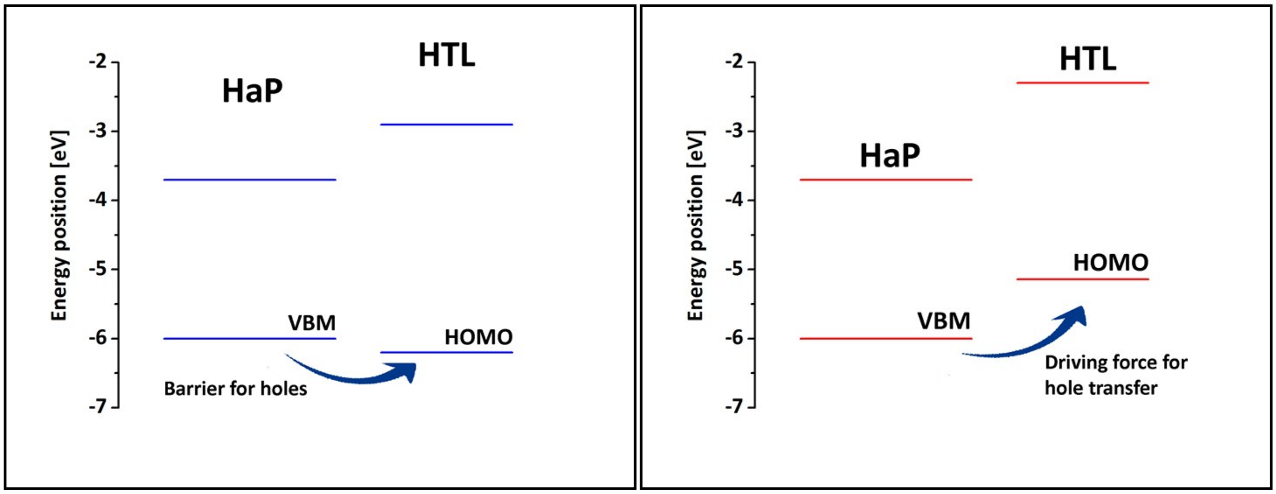

Figure S2. Band diagram illustrating energy level alignment, promoting hole blocking (left) and hole transport (right) between the HaP and organic layer.

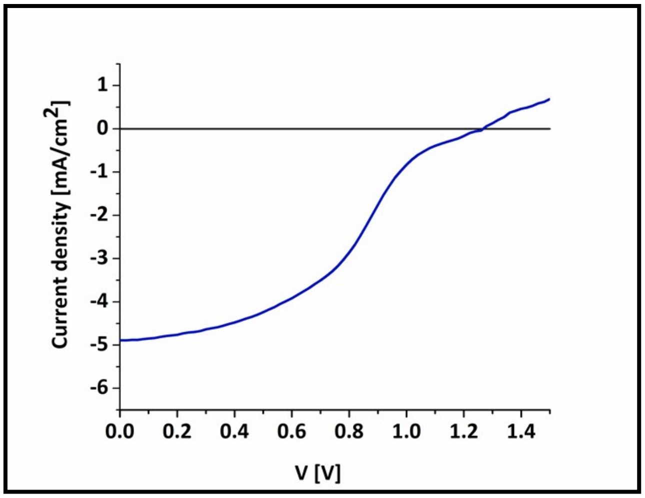

Figure S3. S-shaped I-V curve under illumination of FTO\dTiO$_2$\MAPbBr$_3$(Cl)\CBP\Au, where the CBP is more than 20 nanometers thick on top of the HaP layer.

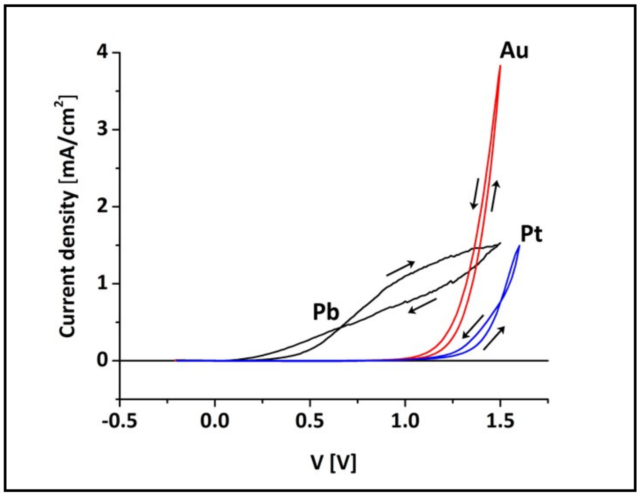

Figure S4. Dark I-V curves of TiO2/MAPbBr3(Cl)/CBP/metal (Pt, Au or Pb). As in the light curve the Pb dark curve show significant hysteresis with respect to Pt and Au.

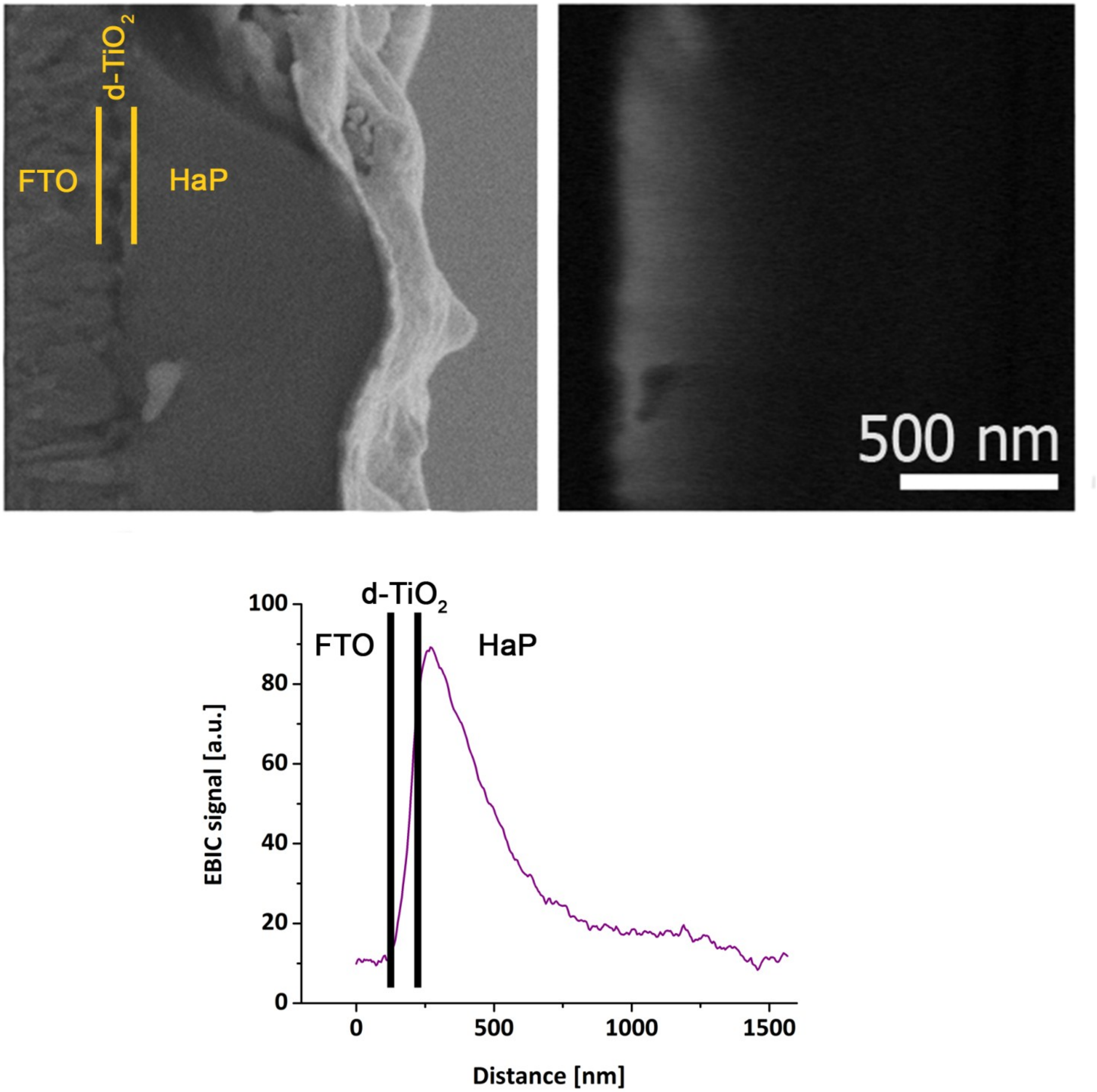

Figure S5. Secondary image (left) and EBIC image (right) and EBIC profile (bottom) of with PMMA.

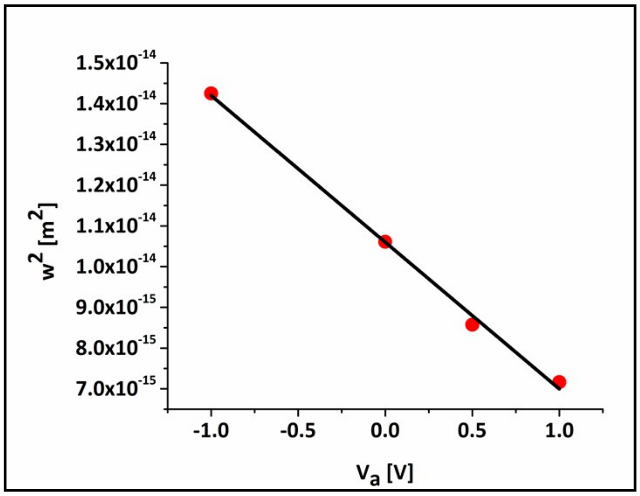

Figure S6. Change of space charge region width with applied bias for glass/FTO/TiO_2/HaP/CBP/Pt device as measured by EBIC. The linear correlation between the W_d^2 and V_a allows to calculate the carrier concentration in the film from the slope of the linear regression, which, in this case, is $N_A = 2 - 3 \times 10^{18}$ cm^{-3}. The estimated error in W_d^2 is smaller than the size of the marker dots.

CPD and SPV detailed working mechanism:

In a Kelvin Probe (KP) measurement the change in capacitance between the (vibrating) probe and the sample surface is nulled. This is done by biasing the probe with respect to the sample so that their vacuum levels align. The applied bias (and the inferred vacuum level difference) is the difference in surface potentials between the probe and the sample and is known as contact potential difference (CPD). In practice the applied bias is the WF difference between the probe and the sample. Thus, by comparing the CPD of a reference sample with a known WF, typically freshly cleaved highly oriented pyrolitic graphite (HOPG, WF = 4.65 eV), with a tested sample, the WF of the latter can be measured. In the dark, electronic equilibrium requires a constant position of the Fermi level throughout the device. Upon illumination charge separation manifested by charge transfer across (an) interface(s) or by compensation for (a) built-in field(s) or both change the electrostatic potential profile [and, thus, the reference (vacuum) level position] across the device and, as a result, the CPD changes.[1] The lower limit of the expected contribution of light-induced changes in potentials at and across interfaces and/or built-in fields to V_{oc} can be deduced from the CPD light response (the surface photovoltage, SPV). The SPV was calculated from the probe-sample contact potential difference (CPD) in the dark and under illumination as $SPV = CPD_{(light)} - CPD_{(dark)}$. After a sample was placed in the glovebox the CPD measurement was started immediately. Samples were allowed to stabilize (either in the dark or under illumination) until the drift was reduced to less than 1 mV/min (usually ~15 min). Light intensity was controlled using a variable transformer and light intensity was calibrated using a Si photodiode (IXYS SolarBIT) placed at the location of the sample. Because of the size and shape of the photodiode, it was not possible to calibrate the light intensity under front illumination with the probe in place. The probe has a transparency of 60% and the light intensity during front illumination was corrected for this transparency. Illumination intensity was increased stepwise until no further change in CPD was induced.

SPV measurements of FTO / TiO_2 / HaP / CBP / carbon:

Devices were fabricated in the same way as described in the experimental section of the main text. The carbon was deposited by thermal evaporation of a carbon filament, creating a ~6 nm thick top contact. The SPV value of this configuration was 1300 ± 100 [mV]. We did not fabricate full devices in this way, since the electrode was too thin and the sheet resistance too large.

Working procedure and data analysis for EBIC:

Samples for EBIC measurements were cleaved to expose the solar cell cross-section and transferred immediately into the SEM chamber. EBIC images were interpreted by simulating the EBIC profiles obtained, using the charge collection model of Donolato to distinguish between the space charge region (SCR) and quasi-neutral region,[2,3] and to measure their extent and the decay rate of the signal in the latter. For low-injection conditions, Donolato described the EBIC signal acquired at a p-n junction as a convolution of a lateral generation profile and a collection function ranging from the edge of the space-charge region (SCR) to the back contact. With the boundary conditions of complete collection in the SCR and translation invariance parallel to the p-n junction, the model is reduced into one dimension (perpendicular to the p-n junction). Each profile to be analyzed is the average of ca. 25 EBIC lines. The diffusion length and W_d were extracted from the averaged profile. The reported value is the result of an average extracted from at least 5 locations across the device.

References

1 L. Kronik and Y. Shapira, *Surf. Sci. Rep.*, 1999, **37**, 1–206.

2 C. Donolato, *J. Appl. Phys.*, 1989, **66**, 4524–4525.

3 N. Kedem, T. M. Brenner, M. Kulbak, N. Schaefer, S. Levcenko, I. Levine, D. Abou-Ras, G. Hodes and D. Cahen, *J. Phys. Chem. Lett.*, 2015, 2469–2476.